Supporting Information

Porous-carbon aerogels with tailored subnanopores for high cycling stability and rate capability potassium ion battery anodes

Wenqi Zhao,[1,2] Yupeng Shen,[2] Hui Zhang,[2] Yunsong Wang,[2] Yizeng Wu,[2] Huaisheng Wu,[2] Mingchu Zou,[2] Qian Wang,[2] Yibin Li,[1*] Anyuan Cao[2*]

[1] National Key Laboratory of Science and Technology on Advanced Composites in Special Environments, Centre for Composite Materials and Structures, Harbin Institute of Technology, Harbin 150080, P. R. China

[2] Department of Materials Science and Engineering, College of Engineering, Peking University, Beijing 100871, P. R. China

*Corresponding authors: Email: anyuan@pku.edu.cn, liyibin@hit.edu.cn

Supporting Information:

Figure S1. SEM and TEM characterizations of materials and control samples.

Figure S2. Incremental pore volume and cumulative pore volume.

Figure S3. Micropore volume ratio and mesopore volume of PCN (air-0.5 h), PCN (air-1 h), and PCN (air-1.5 h).

Figure S4. Horvath-Kawazoe (HK) differential pore volume and Barrett-Joyner-Halenda (BJH) desorption differential pore volume.

Figure S5. XPS characterization.

Figure S6. Raman spectra.

Figure S7. EIS of PCN electrodes were recorded during the first cycle at different states.

Figure S8. XRD patterns of PCN electrodes were tested at different states.

Figure S9. TEM characterizations and elements mapping of PCN (air-1 h) after 5000 cycles.

Figure S10. First three cycles of CV curves for the four samples at 0.1 mV/s.

Figure S11. Capacitive contribution of PCN (air-1 h) from 0.1 mV/s to 0.5 mV/s.

Figure S12. Capacitive contribution of PCN (air-1.5 h) from 0.1 mV/s to 0.5 mV/s.

Figure S13. Capacitive contribution of PCN (air-0.5 h) from 0.1 mV/s to 0.5 mV/s.

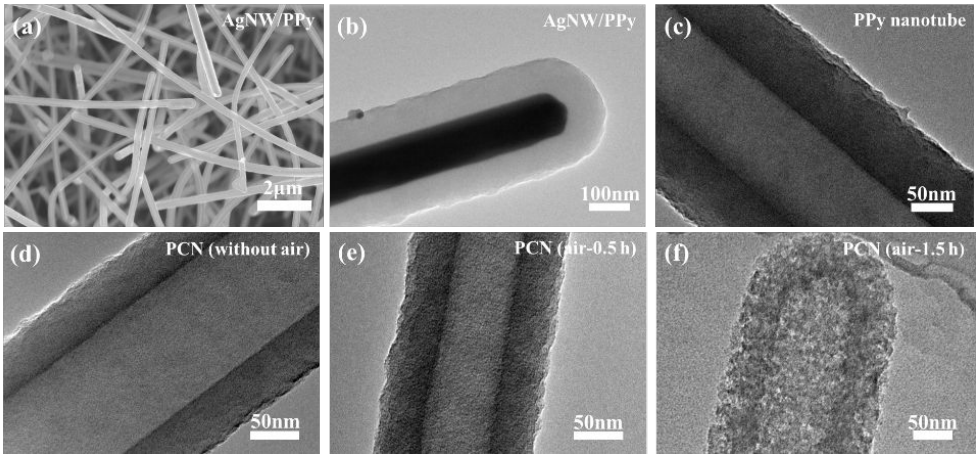

Figure S1. (a) SEM and (b) TEM characterizations of AgNW/PPy, TEM images of (c) PPy nanotube, (d) PCN (without air), (e) PCN (air-0.5 h) and (f) PCN (air-1.5 h).

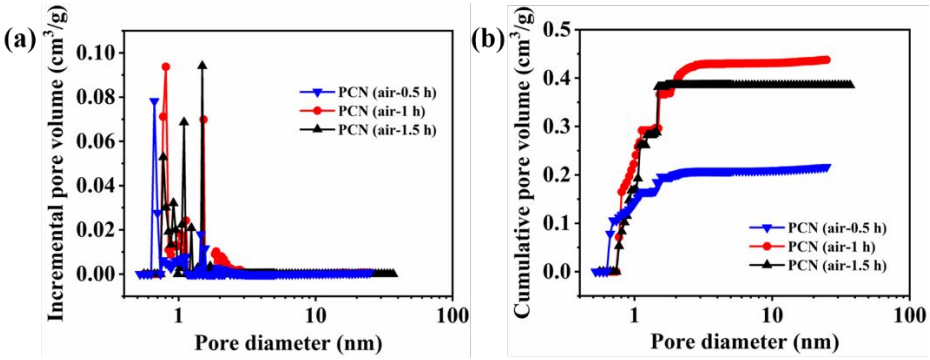

Figure S2. (a) Incremental pore volume and (b) cumulative pore volume of PCN (air-0.5 h), PCN (air-1 h), and PCN (air-1.5 h).

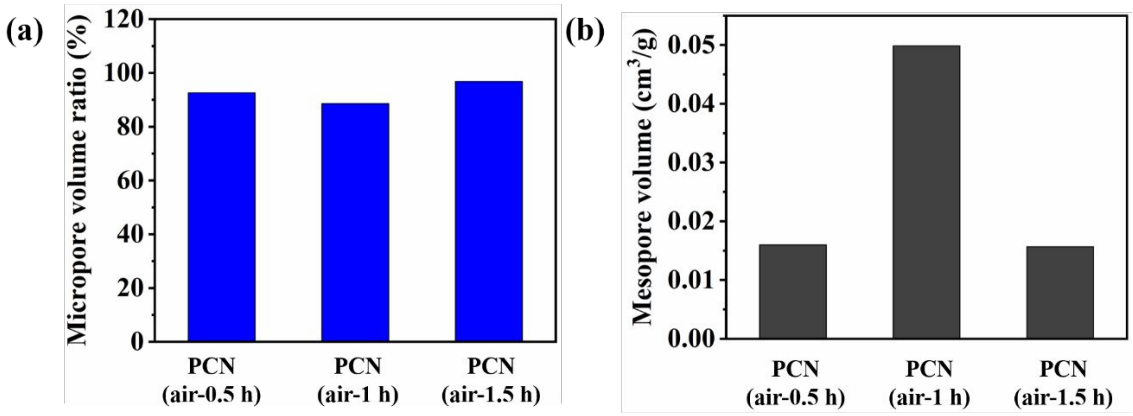

Figure S3. (a) Micropore volume ratio and (b) mesopore volume of PCN (air-0.5 h), PCN (air-1 h), and PCN (air-1.5 h).

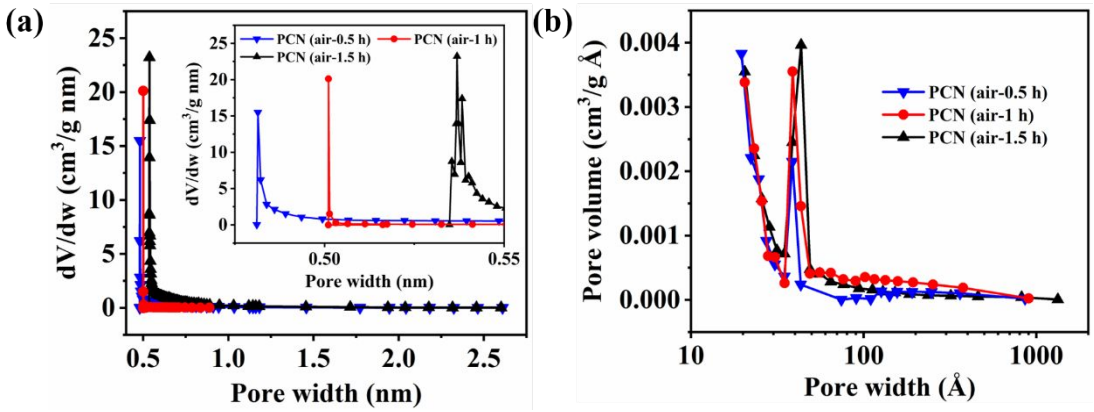

Figure S4. (a) Horvath-Kawazoe (HK) differential pore volume plots of PCN (air-0.5 h), PCN (air-1 h), and PCN (air-1.5 h) show increased pore size and pore volume as the air treatment prolonged. (b) Barrett-Joyner-Halenda (BJH) desorption differential pore volume plots. The corresponding surface area based on BJH method are 67.1 m^2/g (PCN (air-0.5 h)), 93.1 m^2/g (PCN (air-1 h)), 100.3 m^2/g (PCN (air-1.5 h)).

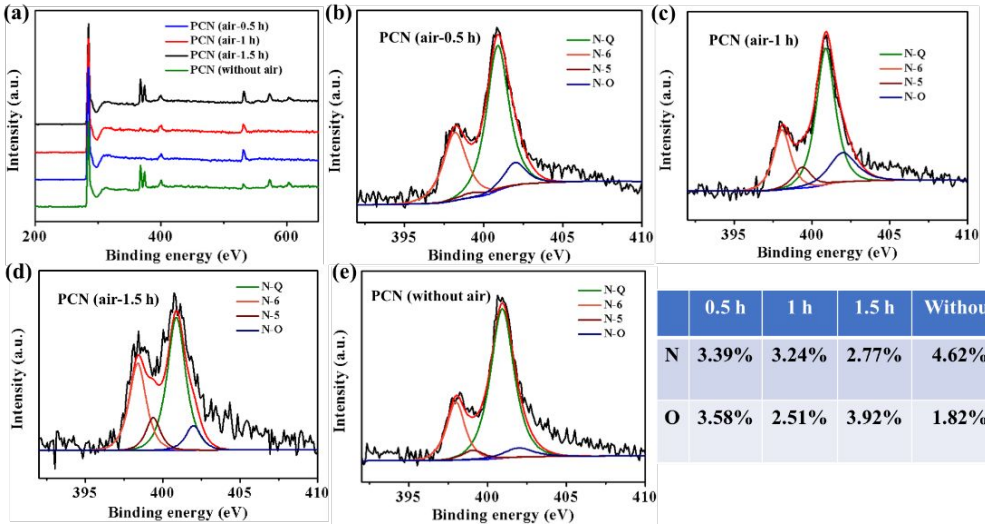

	0.5 h	1 h	1.5 h	Without
N	3.39%	3.24%	2.77%	4.62%
O	3.58%	2.51%	3.92%	1.82%

Figure S5. XPS characterizations. (a) XPS survey spectra of the four samples. (b-e) N 1s XPS spectra of PCN (air-0.5 h), PCN (air-1 h), PCN (air-1.5 h) and PCN (without air), respectively. Table: N and O content of the four samples.

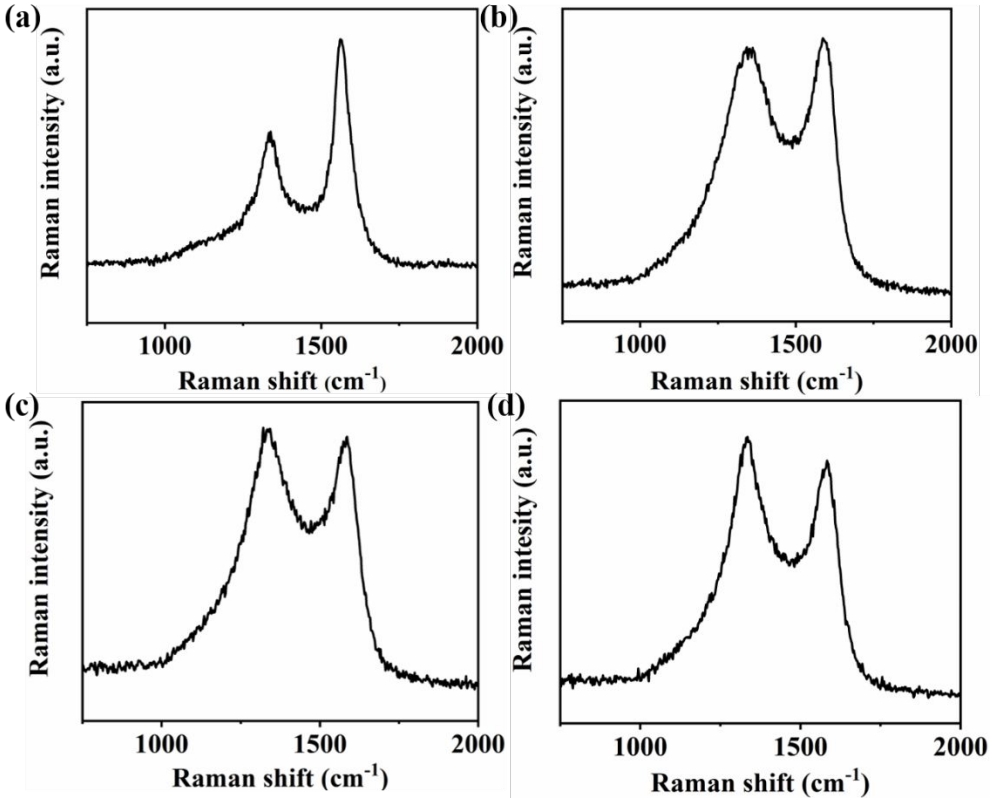

Figure S6. Raman spectra. (a) PCN (without air). (b) PCN (air-0.5 h). (c) PCN (air-1 h). (d) PCN (air-1.5 h).

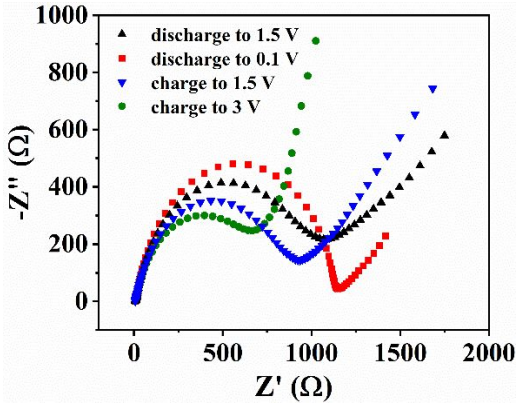

Figure S7. EIS of PCN electrodes were recorded during the first cycle at different states.

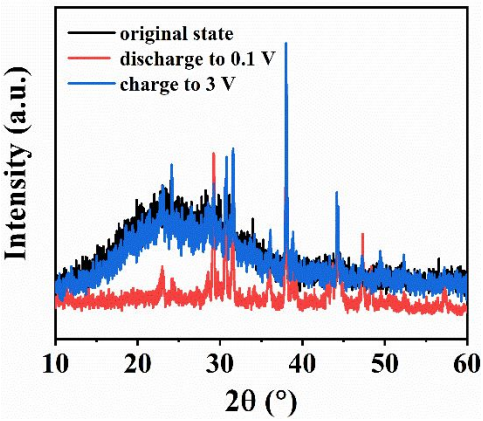

Figure S8. XRD patterns of PCN electrodes were tested at different states.

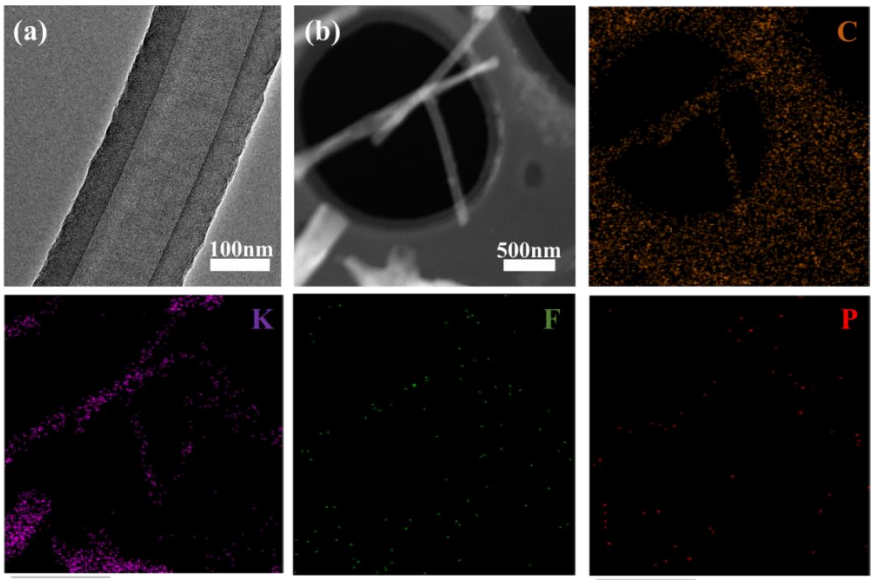

Figure S9. (a) TEM characterizations and (b) elements mapping of PCN (air-1 h) after 5000 cycles at various rates from 70 mA/g to 5 A/g.

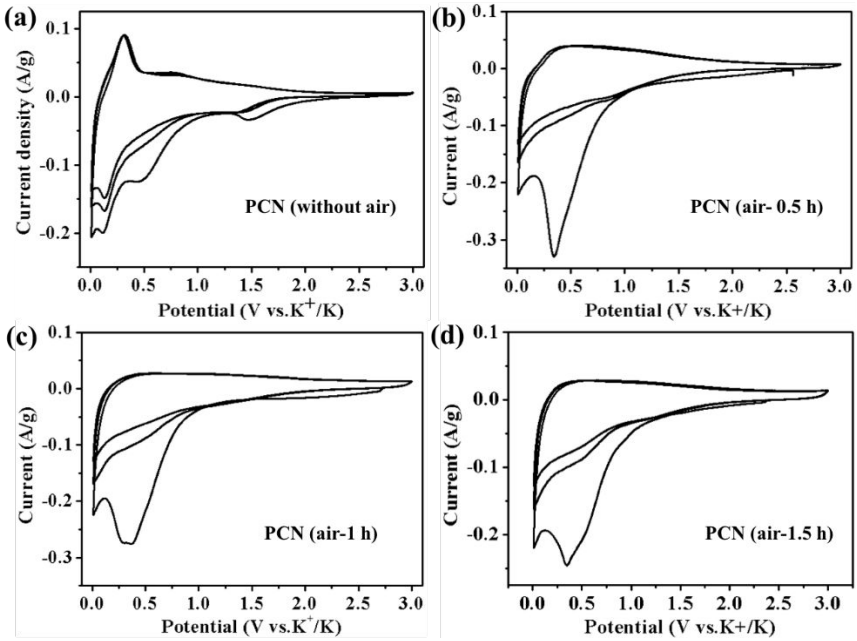

Figure S10. First three cycles of CV curves for the four samples at 0.1 mV/s. (a) PCN (without air). (b) PCN (air-0.5 h). (c) PCN (air-1 h). (d) PCN (air-1.5 h).

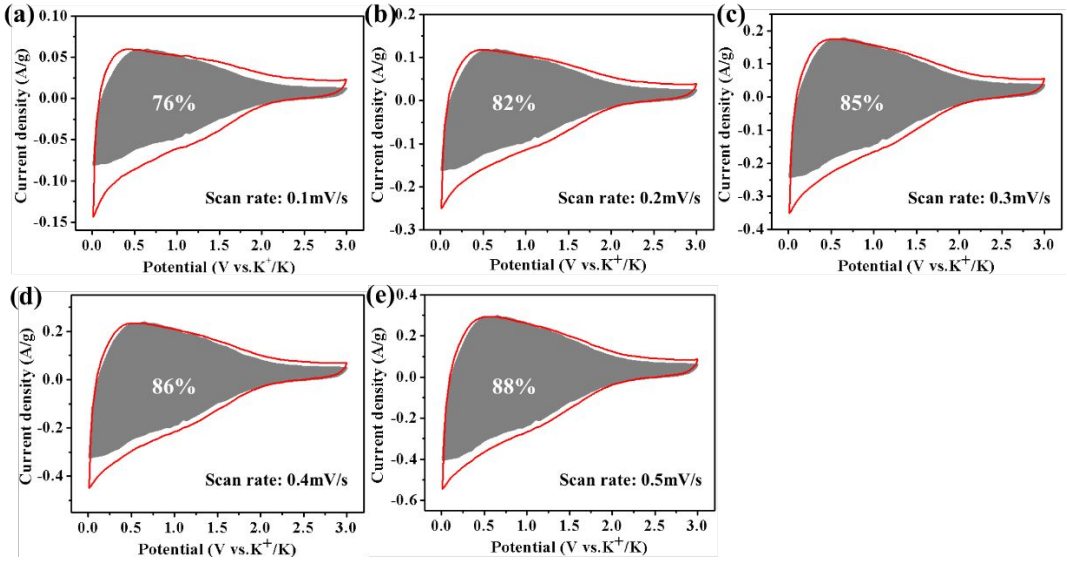

Figure S11. Capacitive contribution of PCN (air-1 h) at (a) 0.1 mV/s, (b) 0.2 mV/s, (c) 0.3 mV/s, (d) 0.4 mV/s, and (e) 0.5 mV/s.

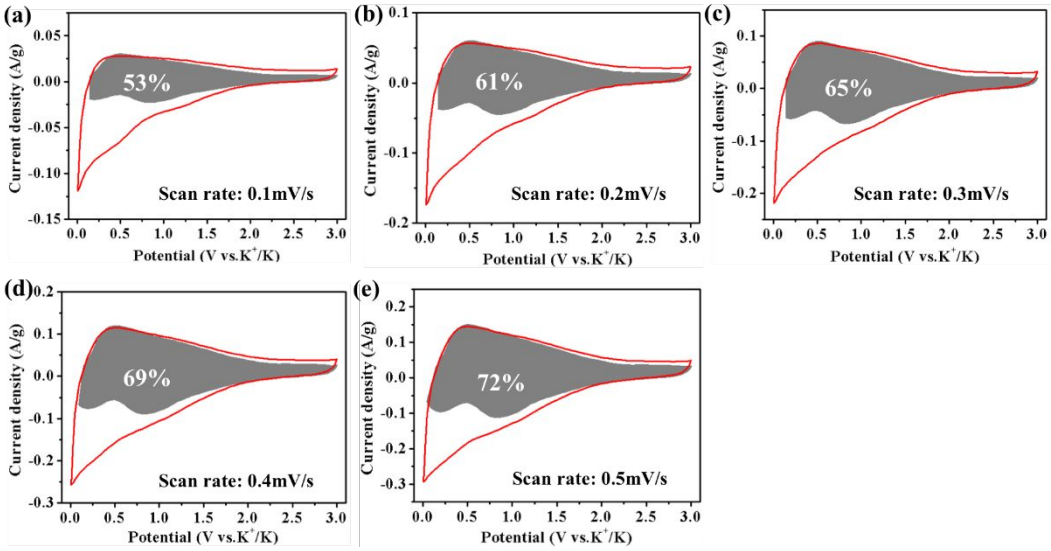

Figure S12. Capacitive contribution of PCN (air-1.5 h) at (a) 0.1 mV/s, (b) 0.2 mV/s, (c) 0.3 mV/s, (d) 0.4 mV/s, and (e) 0.5 mV/s.

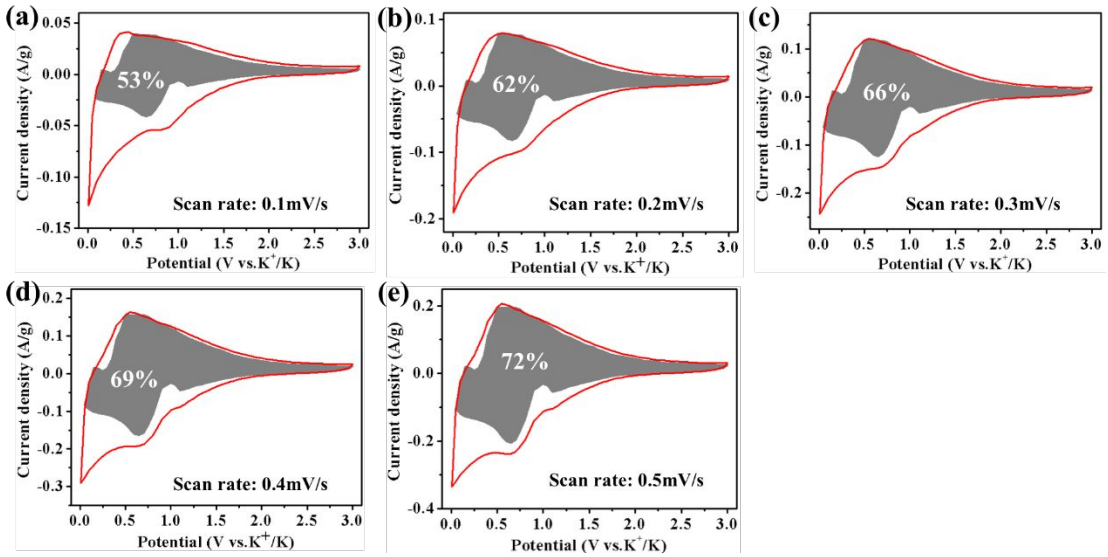

Figure S13. Capacitive contribution of PCN (air-0.5 h) at (a) 0.1 mV/s, (b) 0.2 mV/s, (c) 0.3 mV/s, (d) 0.4 mV/s, and (e) 0.5 mV/s.